VOL. 24, NO. 3, 2025, 263-269
elektrika.utm.my
ISSN 0128-4428

ELEKTRIKA
Journal of Electrical Engineering

Timing Considerations in Blockage Prediction with IRS Beamforming for Ultra-Reliable Network Connectivity

Fu Seong Woon[1] and **Chee Yen Leow**[1*]

[1]Wireless Communication Centre, Faculty of Electrical Engineering, Universiti Teknologi Malaysia, 81310 UTM Skudai, Johor, Malaysia.

[*]Corresponding author: bruceleow@utm.my

Abstract Ensuring ultra-reliable network connectivity in dynamic environments requires accurate and timely blockage prediction. This study analyzes the timing considerations in blockage prediction with Intelligent Reflecting Surface (IRS) beamforming, comparing adaptive filtering techniques—Least Mean Squares (LMS), Normalized Least Mean Squares (NLMS), and Recursive Least Squares (RLS)—against Long Short-Term Memory (LSTM) networks. Results show that LSTM achieves superior accuracy, ranging from 96.40% to 93.21%, while adaptive filters decline over time. Despite its superior accuracy, LSTM incurs a computational delay of 50 µs over the baseline model, which itself is 80 µs slower than adaptive filters. To enhance network reliability, we integrate Intelligent Reflecting Surface (IRS) beamforming, optimizing signal reflections under Non-Line-of-Sight (NLoS) conditions. For a base station (BS) communicating with a 64×64 uniform planar array (UPA) Intelligent Reflecting Surface (IRS), blockage proactive prediction must anticipate at least 31 ms into the future to accommodate transmission delays, handover, and beam training. These findings highlight LSTM's potential in enhancing real-time blockage prediction and real-time network adaptability.

Keywords: Proactive Blockage Prediction, Fifth Generation (5G), Intelligent Reflecting Surface, Beamforming, Ultra-Reliable Network Connectivity, Deep Learning

Article History: received 14 March 2025; accepted 9 September 2025; published 22 December 2025
Digital Object Identifier 10.11113/elektrika.v24n3.700

1. INTRODUCTION

1.1 How early should we predict the blockage

[1] states that a duration of up to 90 ms is insufficient for preemptive measures to mitigate blockages or Non-Line-of-Sight (NLoS) conditions, such as handover or beam training. In contrast, this study demonstrates the ability to predict blockages up to 210 ms in advance when a moving obstacle, such as a person walking across the path between the Base Station (BS) and the receiver, is present. The proposed approach achieves prediction accuracy of 91%.

Figure 1 illustrates the beam coherence time, comparing Baseline and Deep Learning (DL)-based solutions. The total beam training time for all antennas is denoted as T_{tr}. The Baseline approach occupies a significant portion of the beam coherence time (T_B), whereas the proposed DL solution demonstrates a more efficient utilization of this time frame. When $T_{tr} > T_B$, network continuity cannot be guaranteed due to delays in the beamforming process [2]. This work addresses the challenges associated with large surfaces, as discussed in [3], where T_B can serve as a critical bottleneck in beamforming technologies for large antenna arrays.

Works from [1-3] have been summarized that the larger the number of elements of Intelligent Reflecting Surface (IRS), time for BS to perform beamforming is longer. To enable proactive action to be taken, the prediction could be different depending on the size of the IRS. Conventional methods of channel predictions are adaptive filters that are crucial to maintain the capacity of the communication networks, e.g., Least Mean Squares (LMS), Least Squares (LS), Recursive Least Squares (RLS), Kalman Filter (KF) and etc [4].

According to [5], KF is commonly used for non-stationary channel tracking. KF could perform better and respond quickly to parameter changes compared to LS and RLS [6]. Recently [7], is using CNN for channel prediction to maintain capacity at 97% compared to KF Auto Regression (AR), 92.5% with previous channel information to predict the next one in an Orthogonal Frequency-Division Multiplexing (OFDM) Multiple Input Single Output (MISO) system in 3.5Ghz carrier frequency. These latencies present significant bottlenecks for achieving Ultra-Reliable Low-Latency Communication (URLLC), as discussed in [8].

In contrast, ML-based solutions can be trained offline and deployed in real time without depending on feedback, which substantially reduces latency [9]. Recent studies have demonstrated the use of Convolutional Neural Networks (CNNs) for predicting channel conditions in

OFDM-MISO systems, achieving a 97% capacity retention rate compared to 92.5% for KF-based auto-regression models [7].

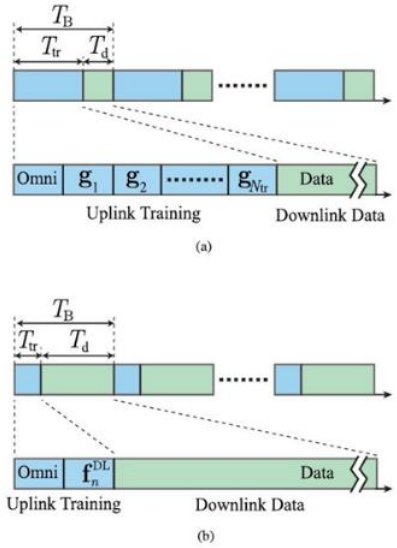

Figure 1. Beam coherence time, T_B, (a) Baseline solution for beamforming by searching for the optimal beam vector. (b) Deep Learning solution for beamforming [2]

Moreover, ML architectures such as Recurrent Neural Networks (RNNs) and Transformers have shown potential in multi-step prediction, further enhancing proactive beamforming capabilities [10, 11].

This paper builds upon these insights and proposes a robust DL-based framework capable of multi-step blockage prediction and efficient beamforming in IRS-assisted mmWave systems. By addressing the limitations of traditional methods and integrating recent advances in ML for wireless communications, we contribute toward enabling more resilient and low-latency wireless networks.

2. SYSTEM MODEL

2.1 Received Signal Model

Consider a communication system represented by our previous work [12], where a BS communicates with a vehicular user with the assistance of an IRS. However, the IRS-user link can be blocked by obstacles, e.g., buses or trucks. For simplicity, we assume that the BS and vehicle user have equipped with a single antenna while the IRS is equipped with M antennas. OFDM based system is adopted with number of subcarriers, K. $\boldsymbol{h_{BU,k}} \in \boldsymbol{C}$ is defined as a direct channel between the BS and the user. In this study, the direct BS–user link is neglected under the assumption that mmWave communication operates in a severe NLoS environment, where large vehicles, buildings, or other obstacles block the LoS path. Given the high path loss and blockage sensitivity of mmWave signals, the direct link contribution is negligible compared to the IRS-assisted path, and thus its omission simplifies the analysis without affecting the model's applicability to realistic deployment scenarios. Then, adopting from [12], $\boldsymbol{h_{B,k}}$ and $\boldsymbol{h_{U,k}} \in \boldsymbol{C^{M\times 1}}$ are defined as uplink channels between BS and user to IRS at the $\boldsymbol{k^{th}}$ subcarrier. By reciprocity, the transpose of the uplink channels, $\boldsymbol{h_{U,k}^T}$ and $\boldsymbol{h_{B,k}^T}$, are downlink channels. The interaction matrix of the $\boldsymbol{k^{th}}$ subcarrier, $\boldsymbol{\Psi_k} \in \boldsymbol{C^{M\times M}}$, is the interaction characteristic of the incident signal from the transmitter at IRS. The transmitted signal, $\boldsymbol{s_k}$ is sent over $\boldsymbol{k^{th}}$ subcarrier from the BS to user which satisfies the total power constraint $\boldsymbol{E|s_k|^2 = P_T/K}$, with $\boldsymbol{P_T}$ as the total transmit power. Then received signal at the user's end with received noise, $\boldsymbol{n_k} \sim \boldsymbol{N_C(0, \sigma_n^2)}$ is expressed as:

$$y_k = \mathbf{h}_{U,k}^{T} \boldsymbol{\Psi_k} \mathbf{h}_{B,k} s_k + \mathbf{h}_{BU,k} \mathbf{s}_k + n_k \quad (1)$$

Since it is assumed that the direct channel is insignificant in this case, it can be disregarded. The receive signal can then be expressed as:

$$y_k = \mathbf{h}_{U,k}^{T} \boldsymbol{\Psi_k} \mathbf{h}_{B,k} \mathbf{s}_k + n_k \quad (2)$$

The diagonal structure of the interaction matrix, $\boldsymbol{\Psi_k}$, may be layered in a reflection beamforming vector, $\psi_k \in \boldsymbol{C^{M\times 1}}$, due to the assumption that only phase shifters implemented in IRS elements are used. The same applied to all subcarriers, $\psi_k = \psi$, $\forall k$. Therefore, it may be expressed in Hadamard product form as follows:

$$y_k = \left(h_{U,k} \circ h_{B,k}\right)^T \psi_k s_k + n_k \quad (3)$$

2.2 Channel Model

In this work, we adopt the same geometric-based wideband channel model as in our previous study, where the channel vector of the u^{th} user at the k^{th} subcarrier is given by:

$$\mathbf{h}_{U,k}^{T} = \sum_{d=0}^{D-1} \sum_{\ell=1}^{L} \alpha_\ell \, e^{-\frac{j2\pi k}{K} d} \, p(dT_s - \tau_\ell) \mathbf{a}(\theta_\ell, \phi_\ell) \quad (4)$$

where L is the total number of channel paths and α_ℓ, τ_ℓ, θ_ℓ, ϕ_ℓ are the ℓ^{th} channel path gains, which include path losses, the delay, the azimuth and elevation arrival angles, respectively. T_S stands for sampling time and D for the length of the cyclic prefix, with the assumption that DT_S is less than the maximum delay. The downlink IRS-user channel $\mathbf{h}_{U,k}$ can be defined similarly. To accomodate for the variations of both channels, $\{\mathbf{h}_{B,k}\}_{k=1}^{K}$ and $\{\mathbf{h}_{U,k}\}_{k=1}^{K}$, over time, we employ a block fading channel model in which the channel is considered to be constant throughout the coherence time, T_C.

3. METHODOLOGY

3.1 Problem Formulation

As discussed in our previous work [11], the IRS plays a crucial role in sensing the environment and predicting blockages in the system. The problem involves anticipating potential blockages in the IRS-user link in the near future. Due to its proximity to the user, the IRS can significantly contribute to sensing the environment and predicting blockages. In this scenario, a single-antenna user transmits a pilot signal to the IRS, utilizing compressed sensing with a machine learning (ML) technique, as proposed in [13]. The receive signal power is

sampled from a few randomly distributed active elements on the IRS. The number of active elements, denoted as $\bar{M}$, is the product of the number of horizontal (M_h) and vertical (M_v) elements. These active elements capture the channel vector of each x-axis coordinate, while the moving vehicle transmits an omni-directional pilot signal using a single antenna to the IRS. The matrix $\mathbf{G}_{IRS}$, an $\bar{M} \times M$ selection matrix, selects entries from the original channel vector corresponding to the IRS active elements. Specifically, $\mathbf{G}_{IRS} = [\mathbf{I}]A$, where A represents the set of indices of the active elements and $\mathbf{I}$ is the identity matrix corresponding to the IRS active elements. The IRS sampled channel vector, $\mathbf{h}_{U,k} \in \boldsymbol{C}^{\bar{M}\times 1}$, at the k_{th} subcarrier is expressed as:

$$\bar{\mathbf{h}}_{U,k} = \mathbf{G}_{IRS}\mathbf{h}_{U,k} \tag{5}$$

Let $\hat{\hat{\boldsymbol{h}}}$ represent the noisy sampled channel vector obtained from the user's pilot signal. It can be expressed as follows, where $\boldsymbol{w_k} \sim \boldsymbol{\mathcal{N}_C}(\mathbf{0}, \boldsymbol{\alpha_n^2 I})$ denotes the noise vector received at the IRS's active elements:

$$\bar{\mathbf{h}}_{U,k} = \mathbf{G}_{IRS}\mathbf{h}_{U,k} + \boldsymbol{w_k} \tag{6}$$

We define $t \in Z$ as the index for discrete time instances, and $f[t] = 0, 1$ represents the link status at the $t - th$ time instance. When, $f[t] = 1$, the link is blocked, meaning the Line of Sight (LoS) route between the transmitter and receiver is obstructed, while $f[t] = 0$ indicates an unobstructed link. At each time instance t, if a single-antenna user transmits a pilot signal to the IRS, the sampled channel vector is captured from a few randomly chosen active IRS elements. These active IRS elements will then receive the pilot signals and estimate the noisy sampled channel vector. The concatenated noisy sampled channel vector at the $t - th$ time interval, $\hat{\hat{\mathbf{h}}}[t]$, is expressed as follows:

$$\hat{\hat{\mathbf{h}}}[t]vec = \left(\hat{\hat{\mathbf{h}}}_{U,1}[t]\,, \hat{\hat{\mathbf{h}}}_{U,2}[t] \ldots\,, \hat{\hat{\mathbf{h}}}_{U,K}[t]\right) \tag{8}$$

To facilitate machine learning (ML) training and avoid data loss, the noisy sampled channel vector is normalized to the range [0, 1] by dividing it by the maximum amplitude of all the channels in the dataset, $\hat{\hat{\boldsymbol{H}}}$. Thus, the normalized noisy sampled channel vector, $\hat{\hat{\mathbf{h}}}_{norm}[t]$, is given by:

$$\hat{\hat{\mathbf{h}}}_{norm}[t]\frac{\hat{\hat{\mathbf{h}}}[t]}{\max \hat{\hat{\mathbf{h}}}[t]} \tag{9}$$

Let T_o represent the observation time window. The sequence of sampled channel vectors from previous time instances within the observation window, $t - T\_o + 1 \ldots, t$, is combined into $S_{uo,h}$, defined as:

$$\mathrm{S_{uo,h}} = \{\hat{\hat{\mathbf{h}}}_{norm}[t+n]\}_{n=1}^{-T_o} \tag{10}$$

Given these inputs, the goal of this study is to predict the future blockage link status at time T_p. B_{T_p} represents the future link status within the $T_p{-}th$ instance, and it is defined as follows:

$$B_{T_p} = \begin{cases} 0, \; if \;\; f[t+n_p] = 0\,, \forall n_p \in \{1, \ldots, T_p\} \\ 1, \; otherwise \end{cases} \tag{11}$$

Where 0 indicates no obstacles and 1 indicates a blockage in front of the IRS. Once the predicted link status $\hat{B}_{T_p}$ is obtained, the objective is to optimize the prediction accuracy and minimize the RMSE by developing appropriate ML models and training them using a sequence of sampled channel vectors.

3.2 Baseline of Pre-blockage Receive Signal Power for Blockage Prediction

For comparison, the baseline is adopted from [14]. The received signal, without noise, at the Fully-active IRS from the user's pilot signal with a single antenna at time instance t is defined as follows, where mmm represents each IRS element:

$$r_{k,m}[t] = \mathbf{h}_{U,k}^{T}[t]\psi_k s_k[t] + n_k \tag{12}$$

The total power over K subcarriers is then given by:

$$|r_m[t]|^2 = \sum_{k=1}^{K}\left|r_{k,m}[t]\right|^2 \tag{13}$$

At the $t - th$ instance, the receive power vector for $\boldsymbol{M}$ beams is defined as:

$$\boldsymbol{r}[t] = \boldsymbol{vec}[|r_1[t]|^2 \ldots |r_M[t]|^2]^T \tag{14}$$

Since the user's antenna has $\boldsymbol{E}$ number of antennas, the total receive power from multiple antennas for $\boldsymbol{M}$ beams is the sum of the receive powers:

$$\boldsymbol{r}[t] = \sum_{e=1}^{E}\boldsymbol{r}_e[t] \tag{15}$$

Similar to Equation (10), the sequence of the receive power vector for these beams is defined as:

$$S_{uo,r} = \{\boldsymbol{r}[t+n]\}_{n=1-T_o}^{0} \tag{16}$$

Finally, Equation (11) is used to predict the future blockage link status within the $T_p - th$ instance, B_{T_p}.

3.3 Machine Learning Models

Building on the work in [14], this study employs an IRS with a limited number of active elements and utilizes both types of Recurrent Neural Networks (RNNs) with Gated Recurrent Units (GRU) and Long Short Term Memory (LSTM) for predicting future link blockages. These models are capable of accurately predicting blockages with low RMSE before a Non-Line-of-Sight (NLoS) condition occurs. As mentioned in [14], a pre-blockage wireless signature can often be observed in the received power, which can be leveraged to forecast future blockages. Therefore, machine learning can use the sequence of receive signal power to predict potential NLoS conditions between the IRS and the user. This wireless signature is

proposed as a tool for forecasting future link blockages in mmWave systems. Given the complexity of these signatures, machine learning is employed to learn and make use of these patterns. To further investigate this area of blockage prediction, we also incorporate the sequence of channel vectors along with Instantaneous Channel State Information (ICSI) for a performance comparison.

To enable the neural network to learn the time-dependent patterns of observed receive signal power, the GRU network design shown in Figure 2 of [14] is applied with some modifications. The model initially consists of a GRU with q-layers, followed by fully connected feedforward layers, including the output layer. However, in this case, the activation function of the prediction component is changed to linear, rather than the typical rectified linear unit (ReLU). This design can also be applied to the LSTM model by replacing the GRU layers with LSTM layers in the q-layers. For the blockage prediction task, we use the Mean Squared Error (MSE) loss function as the training objective:

$$l_{MSE} = \sum_{t=1}^{T}(p_t - \hat{p}_t)^2 \tag{17}$$

where p_t and $\hat{p}_t$ are the blockage probability of the link status. There are two link statuses, 0 and 1. Then, RMSE is defined as below:

$$RMSE = \sqrt{l_{MSE}} \tag{18}$$

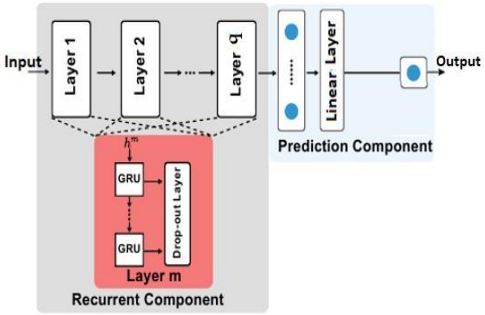

Figure 2. The adopted GRU architect model to predict the link status [14]

Let S denote the total of the sample size. Hence, accuracy can be calculated as below:

$$\text{Accuracy} = \frac{1}{S}\sum_{s=1}^{S}\mathbb{1}\left(B_{T_p}^{(s)} = \hat{B}_{T_p}^{(s)}\right) \tag{19}$$

where $\mathbb{1}$ is the indicator function, and $B_{T_p}^{(s)}$ and $\hat{B}_{T_p}^{(s)}$ $ are the target link status and predicted link status for future time instances of T_p in the problem respectively.

3.4 ViWi Datasets and scenarios

We follow the experimental setup described in [15] to train a deep learning model for blockage detection and prediction in an urban environment. In this scenario, two buses become immobile during rush hour, acting as obstacles between the moving vehicles and the IRS. The BS is located at a traffic light, while the IRS is placed in the middle of the road. The moving vehicle is assumed to travel at 32.04 km/h, transmitting omnidirectional pilot signals with a single antenna. The dataset, named "colo_cam_blk" is generated using the ViWi framework as shown in Figure 3 and consists of high-fidelity synthetic wireless data created with ray-tracing software, Remcom Wireless Insite.

To evaluate the model, 10% of the total 5000 samples are reserved for testing, while the remaining 90% is split into training (70%) and validation (20%) sets. The IRS is configured with a Uniform Planar Array (UPA) structure, consisting of a $\mathbf{8} \times \mathbf{8}$ array with 64 antennas, operating at mmWave 60 GHz. The spacing between antenna elements is half the wavelength of the operating frequency. The experiment is carried out with fully active surface with on the array, hence, 64 active elements for simplification on the setup. A summary of the parameters used in the ViWi dataset is provided in Table 1. This setup is used to predict and detect potential future blockages between the IRS and the moving vehicle's user.

3.5 Adaptive Filters and Beam Training for Blockage Prediction

Adaptive filters are dynamic systems that adjust their parameters in real-time to optimize performance based on changing input signals. They are commonly used in signal processing tasks such as noise reduction, echo cancellation, and system identification. Unlike fixed filters, adaptive filters continuously adapt to the input data by minimizing a cost function, often using algorithms like Least Mean Squares (LMS), Recursive Least Squares (RLS) and Normalized Least Mean Squares (NLMS). This ability to self-tune makes them highly effective in environments with variable conditions, such as wireless communication and speech processing.

According to [3], and as shown in Figure 4, the beam coherence time T_B is defined as:

$$T_B = \frac{D}{v \sin \alpha}\frac{\Theta}{2} \tag{20}$$

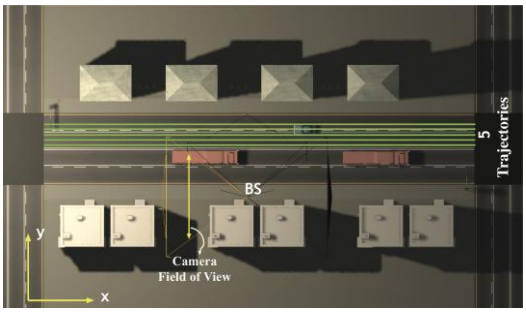

Figure 3. The selected scenario, "colo_cam_blk", in ViWi Dataset Generation Framework [15]

Table 1. The ViWi Dataset Parameters

Dataset Parameter	Value
Frequency band	60 GHz
Active IRS	1
Number of IRS Antennas, (Mx, My, Mz)	(8, 1, 8)
Active users	From 1 to 5000
System bandwidth	125MHz
Number of OFDM subcarriersr	64
Number of OFDM sampling factor	1
Number of OFDM limit	64
Number of channel paths	{1, 20}
Antenna spacing	0.5λ

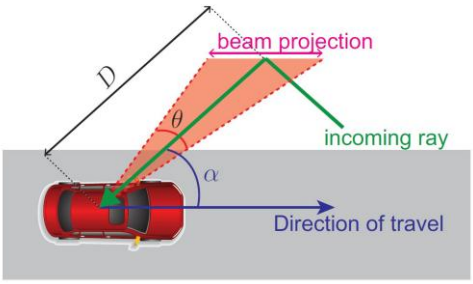

Figure 4. An illustration of the beam coherence time concept [3].

[2] assumes each beam training takes 10 μs. For a single-antenna base station (BS) communicating with a 64×64 uniform planar array (UPA) IRS, the process takes approximately 41 ms. However, when the vehicle is traveling at 80 km/h, the computed T_B is just 10.8 ms. Considering additional factors such as transmission delays, handover time [3], and beamforming training time, the blockage prediction algorithm must anticipate at least 31 ms ahead, equivalent to $T_P = 7.5$, to maintain network reliability and ensure seamless connectivity.

The selection of 31 ms as the minimum prediction horizon is dictated by the timing constraints inherent to beamforming operations in high-frequency mmWave systems. In the proposed system model, the total beam training and reconfiguration time $TtrT_\{\backslash mathrm\{tr\}\}$Ttr is 41 ms, while the beam coherence time $TBT_\{\backslash mathrm\{B\}\}$TB —the duration for which a beam direction remains valid under typical mobility and environmental dynamics—is 10.8 ms. Consequently, the minimum prediction horizon is determined as:

$$T_{pred} \geq T_{tr} - T_B = 41ms - 10.8ms \approx 30.2ms \quad (21)$$

A value of 31 ms is adopted to incorporate a safety margin that accounts for processing latency in prediction modules, residual misalignment in beam tracking, and uncertainties due to mobility and environmental variations. This threshold ensures that the system can detect impending blockages or NLoS conditions, identify suitable alternative beams or handover targets, and complete reconfiguration before the current beam path deteriorates. Selecting a horizon shorter than 31 ms would risk initiating beam adaptation after the coherence window has expired, leading to potential link outages or QoS degradation. Thus, the 31 ms value is not arbitrary but emerges from the fundamental timing gap between beam adaptation latency and beam coherence duration.

With a total number of elements of N_a, and assuming an incident angle $\alpha = 60°$ and a distance $D = 15$m, the azimuth beamwidth Θ can be approximated using the beamwidth formula for a uniform linear array of size $\sqrt{N_a}$, given by:

$$\Theta \approx 0.886 \times \frac{2}{\sqrt{N_a}} \quad (22)$$

where the antenna spacing is set to half the wavelength. This relationship highlights the impact of antenna array size on beamforming precision, reinforcing the necessity for accurate blockage prediction to ensure continuous and stable network performance [3].

4. RESULT AND DISCUSSION

In this comparison, an 8x8 Fully Active IRS is used to receive pilot signals from the user, with an observed time sequence $T_o = 16$ as per [14]. The comparison of accuracy between adaptive filtering methods and machine learning models as shown in Figure 5, particularly LSTM networks, highlights the superior performance of LSTM-based approaches in predictive accuracy. The results from the study show that the proposed LSTM model consistently outperforms adaptive filtering techniques such as Least Mean Squares LMS, NLMS and RLS, as well as a baseline model.

The proposed LSTM model exhibits the highest accuracy across all test cases, with values ranging from 96.40% to 93.21%. The baseline model also performs well but remains consistently lower than the LSTM, with accuracy values ranging from 95.30% to 92.51%. The difference in accuracy between the LSTM and the baseline model suggests that incorporating deeper learning methodologies significantly enhances prediction capabilities over traditional approaches.

Among the adaptive filtering techniques, the LMS algorithm shows the weakest performance, with accuracy decreasing from 79.17% to 65.35%. The NLMS algorithm exhibits slightly better performance compared to LMS, with values fluctuating between 83.84% and 78.76%, indicating improved adaptability. The RLS algorithm, which is typically more computationally intensive, does not surpass NLMS in accuracy. Its values range from 82.42% to 64.84%, demonstrating a downward trend similar to LMS.

All adaptive filtering methods show a decline in accuracy as the dataset progresses, which suggests a potential issue with their ability to generalize over time. In contrast, LSTM and the baseline model show a more gradual decrease in accuracy, implying that they maintain stability over an extended range of inputs. The gap between LSTM and adaptive filters increases over time,

further highlighting the robustness of machine learning-based approaches in handling complex data patterns. Additionally, as the T_p moves further into the future for prediction, accuracy consistently decreases across all models. This trend indicates the increasing difficulty of making long-term predictions due to accumulating uncertainties and complex variations in the data.

Another critical factor in evaluating prediction models is the time required for computation. Figure 6 shows proposed LSTM model takes an average of 50 µs longer than the baseline model to generate a prediction. Meanwhile, the baseline model itself is approximately 80 µs slower than adaptive filtering methods. This indicates that while LSTM provides superior accuracy, it comes at the cost of increased computational time. In real-time applications where rapid predictions are necessary, adaptive filtering methods remain advantageous in terms of speed, despite their lower accuracy. However, in scenarios where accuracy is prioritized over computation time, the LSTM model remains a compelling choice. Future research should consider optimizing LSTM architectures to reduce computational latency while maintaining high predictive performance.

Compared to GRU and adaptive filtering methods, the proposed LSTM model demonstrates superior accuracy, particularly for datasets with long-term dependencies and non-linear temporal patterns. Adaptive filters, being linear and memory-limited, struggle to capture the evolving, non-stationary relationships present in the data, resulting in a sharper decline in accuracy over time. GRU, while more computationally efficient, has a reduced gating complexity that can limit its ability to retain information over extended sequences, leading to slightly lower accuracy than LSTM in datasets where long-range context is crucial. The LSTM's architecture, with separate memory and gating mechanisms, allows it to effectively preserve relevant historical information and adapt to gradual shifts in data distribution, thus maintaining predictive stability as the dataset progresses.

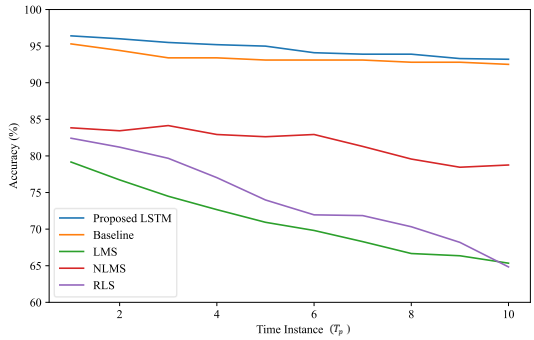

Figure 5. Blockage prediction accuracy comparison of adaptive filters, the Baseline (GRU) and our proposed LSTM against time instance, T_p

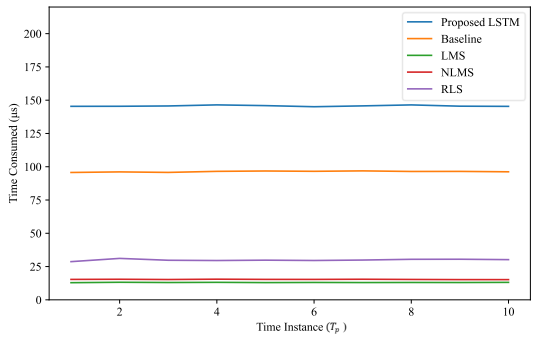

Figure 6. Blockage prediction time consumption comparison of adaptive filters, the Baseline (GRU) and our proposed LSTM against time instance, T_p

5. CONCLUSION

To enhance the reliability of network-based predictions and improve overall system performance, IRS beamforming can be integrated into blockage prediction frameworks. IRS technology enhances wireless communication by dynamically adjusting the phase shifts of reflective elements to optimize signal propagation, mitigating blockages and signal degradation. The use of IRS-assisted beamforming can improve network robustness by rerouting signals through reflective surfaces, reducing the impact of obstructions on real-time data transmission.

The findings suggest that machine learning techniques, particularly LSTMs, provide superior accuracy and stability compared to traditional adaptive filters. While adaptive filtering methods such as LMS, NLMS, and RLS are commonly used in signal processing applications, their declining accuracy highlights their limitations in handling dynamically changing data environments. The consistently high accuracy of LSTM models supports their suitability for predictive tasks where precision is critical. Given the performance trends observed, future research should consider hybrid models that integrate machine learning with adaptive filters to leverage the strengths of both methodologies. Additionally, exploring computational efficiency, real-time processing capabilities, and network reliability through IRS-based enhancements can further improve the practical application of these models.

By incorporating IRS with machine learning models like LSTM, network reliability can be significantly improved, as the system can dynamically adapt to environmental changes and optimize predictive accuracy in response to network fluctuations. This synergy between IRS and deep learning-based prediction models offers a promising solution for enhancing signal stability in high-mobility and complex communication environments. Future research should explore hybrid approaches that combine IRS beamforming with adaptive filtering techniques to improve both accuracy and efficiency in blockage prediction.

ACKNOWLEDGEMENT

This work was supported by the Ministry of Higher Education Malaysia through the Higher Institution Centre of Excellence (HICOE) Grant 4J636 and in part by EU HORIZON MSCA-SE project TRACE-V2X under Grant Agreement No. 101131204.

REFERENCES

[1] Hersyandika, R., Miao, Y. and Pollin, S. Guard Beam: Protecting mmWave Communication through In-Band Early Blockage Prediction, 2022. doi:10.48550/ARXIV.2208.06870. URL https://arxiv.org/abs/2208.06870.W.-K. Chen, *Linear Networks and Systems* (Book style). Belmont, CA: Wadsworth, 1993, pp. 123–135.

[2] Alkhateeb, A., Alex, S., Varkey, P., Li, Y., Qu, Q. and Tujkovic, D. Deep learning coordinated beamforming for highly-mobile millimeter wave systems. IEEE Access, 2018. 6: 37328–37348.

[3] Va, V., Choi, J., Shimizu, T., Bansal, G. and Heath, R. W. Inverse multipath fingerprinting for millimeter wave V2I beam alignment. IEEE Transactions on Vehicular Technology, 2017. 67(5): 4042–4058.

[4] Haykin, S. S. *Adaptive filter theory*. Pearson Education India. 2002.

[5] Abdul Careem, M. A. and Dutta, A. Real-time Prediction of Non-stationary Wireless Channels. IEEE Transactions onWireless Communications, 2020. 19(12): 7836–7850. doi:10.1109/TWC.2020.3016962.

[6] Arnold, M., Miltner, W. H., Witte, H., Bauer, R. and Braun, C. Adaptive AR modeling of nonstationary time series by means of Kalman filtering. IEEE transactions on bio-medical engineering, 1998. 45(5): 553–62.

[7] Lee, H., Jeong, J. and Wang, Z. Deep Learning for Wireless Dynamics. arXiv preprint arXiv:2203.05874, 2022.

[8] She, C., Sun, C., Gu, Z., Li, Y., Yang, C., Poor, H. V. and Vucetic, B. A Tutorial on Ultrareliable and low-latency communications in 6G: integrating domain knowledge into deep learning. Proceedings of the IEEE, 2021. 109(3): 204–246.

[9] Kim, H., Kim, S., Lee, H., Jang, C., Choi, Y. and Choi, J. Massive MIMO channel prediction: Kalman filtering vs. machine learning. IEEE Transactions on Communications, 2020. 69(1): 518–528.

[10] S. K. Dehkordi, M. Kobayashi, and G. Caire, "Adaptive beam tracking based on recurrent neural networks for mmWave channels," *arXiv preprint arXiv:2108.04548*, 2021. [Online]. Available: https://arxiv.org/abs/2108.04548

[11] Z. Albataineh, "Recurrent neural networks for enhanced beamspace channel estimation in mmWave massive MIMO systems," *Wireless Personal Communications*, vol. 140, no. 3, pp. 1241–1258, May 2025. [Online]. Available: https://doi.org/10.1007/s11277-025-11767-7

[12] F. S. Woon and C. Y. Leow, "Intelligent reflecting surfaces aided millimetre wave blockage prediction for vehicular communication," in 2022 IEEE 6th International Symposium on Telecommunication Technologies (ISTT). IEEE, 2022, pp. 11–15.

[13] Taha, A., Alrabeiah, M. and Alkhateeb, A. Enabling large intelligent surfaces with compressive sensing and deep learning. IEEE Access, 2021. 9: 44304–44321.

[14] Wu, S., Alrabeiah, M., Chakrabarti, C. and Alkhateeb, A. Blockage prediction using wireless signatures: Deep learning enables real-world demonstration. arXiv preprint arXiv:2111.08242, 2021.

[15] Alrabeiah, M., Hredzak, A., Liu, Z. and Alkhateeb, A. Viwi: A deep learning dataset framework for vision-aided wireless communications. 2020 IEEE 91st Vehicular Technology Conference (VTC2020-Spring). IEEE. 2020. 1–5.